Bending crush behavior of foam-filled sections

Sigit Santosa*, John Banhart, Tomasz Wierzbicki***
* Impact & Crashworthiness Laboratory, Massachusetts Institute of Technology
Room 5-218, Cambridge, MA-02139, USA
** Fraunhofer-Institute for Manufacturing and Advanced Materials
Wiener Str. 12, 28359 Bremen, Germany

Abstract

Bending crush behavior of thin–walled columns filled with closed–cell aluminum foam is studied experimentally and numerically. Non linear dynamic finite element code was used to simulate quasi–static three point bending experiments. Two strengthening mechanisms are observed. First, the aluminum foam filler retards inward fold formation in the compressive flange, therefore preventing the drop in load carrying capacity due to sectional crush. Then, the inward fold retardation changes the crushing mode from single stationary fold, a typical bending crush behavior of an empty beam, to multiple propagating folds. The progressive fold formations spread plastic deformations, thus dissipating more energy. These phenomena are captured from both experiments and numerical simulations. High bending resistance is also maintained when the foam is placed only locally in the zone of high bending moment. The concept of the effective foam length is then developed, and potential applications of foam–filled sections for crashworthy structures are suggested.

1 Introduction

One fundamental building block that contributes to the crashworthiness of space frame structures is a thin–walled prismatic member. Of interest in the problem of a deep plastic collapse of the thin–walled member under bending are the ultimate strength and energy absorption. The bending resistance of an empty thin–walled beam typically drops very significantly after reaching the ultimate value at a small rotation. The decrease of load carrying capacity is due to inward fold formation at the compression flange, significantly reducing cross sectional area at the crush zone. This typical behavior has been studied by, among others, Kecman [1], McGregor et al. [2], Wierzbicki et al. [3].

Recent development in the manufacturing of metallic cellular materials, such as closed–cell aluminum foams, has increased their potential for use in reinforcing thin–walled column beams. The closed–cell aluminum foam is chosen as an ultralight metal core, since it has a high crushing resistance to weight ratio [4]. The aluminum foam filling is intended to prevent or retard the sectional crush. A pilot study on planar bending response of thin–walled beams with a lightweight metal filler was recently computed by Santosa [5]. It has been shown through numerical and experimental studies that the axial resistance of a thin–walled column is improved dramatically by filling it with the aluminum foam [6], [7].

The objective of the present work is to study the bending response of thin–walled beams filled fully or

J. Banhart, M.F. Ashby, N.A. Fleck: *Metal Foams and Porous Metal Structures.* © MIT Verlag (1999)

partially with closed cell aluminum foams experimentally and numerically. Of interest are the ultimate bending strength and moment–rotation response of the filled beam. Numerical studies were performed at the Impact & Crashworthiness Lab MIT, while experimental tests were conducted at the Fraunhofer Institute For Applied Materials Research (IFAM) in Bremen, Germany. Non linear dynamic finite element code PAM Crash was used to simulate quasi–static three point bending experiments.

2 Specimen preparation and material characterization

The thin–walled beam material is stainless steel Cr18Ni8. The geometry of the square beam is: length $L = 470\ mm$, wall thickness $t = 1.5\ mm$, and square cross sectional width $b = 40\ mm$. The thin–walled beam was made from a thin sheet which was cold formed to produce a square welded seam profile.

Four tensile tests were performed on ZWICK–1476 testing machine to obtain stress–strain characteristics of the steel wall. The specimens were taken parallel to the axial direction of the thin–walled beam. The tests were conducted in room temperature, and the engineering stress – strain characteristics of the steel column are shown in Figure 1.

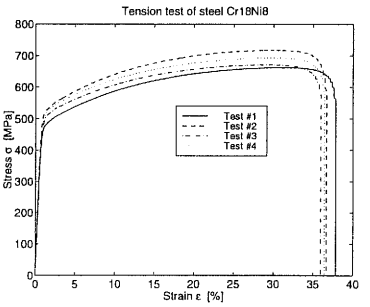

Figure 1: Steel box beam: uniaxial tension behavior

3 Experimental set up

The experimental set up and the three point bending test geometry are shown in Figure 2. Seven bending specimens were prepared with beam cross section 50 x 50 x 1.5 mm and the foam densities varied from 0.6 to 0.835 g/cm^3. The aluminum foam was loosely fitted into the empty space of the square beams. Five beams were fully filled, while two specimens were partially filled with the aluminum foam. Quasi static three point bending experiments were carried out in ZWICK-1476 machine. The punch velocity was set to 0.15 mm/s, and the data acquisition was recorded at a constant rate of 1 Hz.

4 Finite element modeling

The explicit dynamics non-linear finite element code PAM CRASH 98 was used to numerically simulate the axial crushing process of foam–filed columns. The finite model was created by mesh generator

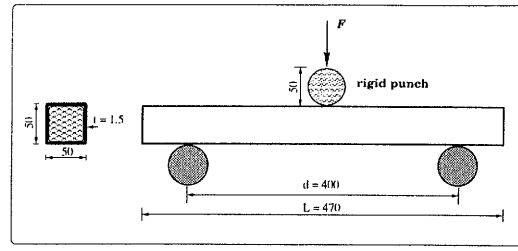

Figure 2: Three point bending test geometry

program HYPERMESH 2.1. The finite element model was then completed with the pre–processor PAM GENERIS. Actual calculations were performed on a SGI Octane workstation with 250 MHz R1000 dual processors. The post–processor PAM VIEW was used for visualization.

Square box column with cross sectional geometry 50 x 50 x 1.5 mm and length 470 mm is considered in the analysis. The column wall was modeled with a *Belytschko–Tsay* 4–node thin shell element. Due to the localized nature of the deformation, the center segment where the bending collapse is expected was modeled with finer mesh size (2.5 x 2.5 mm). The aluminum foam core was modeled with an 8–node solid element. A coarser mesh was chosen for the solid element to reduce computation time.

The punch was modeled by using a finite rigid cylinder with radius $r = 25\ mm$ and length $l = 150\ mm$. Similar cylinder was used in the testing program. Velocity boundary conditions were applied on the rigid punch. The velocity profile was ramped during the first 50 milliseconds to 1 m/s, and then this velocity was held constant. The two stoppers were spaced 400 mm apart and modeled as a stationary rigid cylinder. The friction coefficient between the rigid cylinders and the column wall was treated as a parameter of the process which is varied with the values $\mu = 0.0, 0.1$, and 0.2.

The interaction between the foam and the wall was simulated with a surface–to–surface sliding contact. Frictionless contact condition is assumed on the foam–wall interface. This assumption was found to be appropriated since the adherence between the foam and the column wall was not so dominant [9]. No adhesive bonding was introduced in the simulation.

5 Material modeling

5.1 Thin–walled beam

The constitutive behavior of the thin shell element for the thin–walled beam material was based on the elastic-plastic material model with Von Mises's isotropic plasticity algorithm. The transverse shear effect was considered by this material model. Plastic hardening was based on the polygonal curve definition, in which pairs of the plastic tangent modulus and the plastic stress were specified.

The thin–walled beam material is stainless steel Cr18Ni8 with mechanical properties obtained from the tension test described in Figure 1. Mechanical properties of the thin–walled beam used in the numerical simulations are Young's modulus $E = 2\ 10^5 N/mm^2$, initial yield stress $\sigma_y = 507.6 N/mm^2$, ultimate strength $\sigma_u = 698.6\ MPa$, Poisson's ratio $\nu = 0.3$, and the power law exponent $n = 0.26$.

5.2 Aluminum foam core

Mechanical behavior of aluminum foam is characterized by elastic modulus E^*, plastic collapse stress σ^*_{pl}, shear modulus G^*, plastic shear strength τ^*_{pl}, and densification strain ϵ_D. These parameters strongly depend on the aluminum foam density ρ^*. A complete mechanical properties of aluminum foams is described in Ref. [11].

PAM CRASH offers material modeling for metallic cellular solids capable of undergoing large strain deformation such as aluminum foam. The mechanical properties of the aluminum foam are smeared in three orthogonal directions (x_1, x_2, x_3), see Figure 3. In the case of aluminum foam material, all

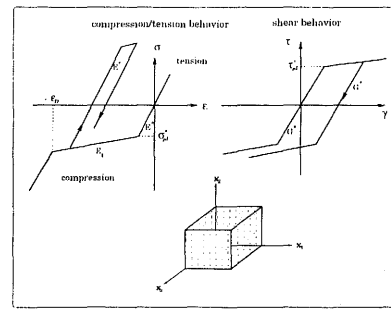

Figure 3: Material modeling of aluminum foam

three orthogonal directions have the same mechanical behavior, i.e. cubic symmetry. Currently, no interaction between components of the stress tensor is incorporated in the yield condition.

6 Experimental and numerical results

6.1 Deformation pattern

Figure 4 show the deformation pattern of the empty thin-walled beam. The deformation pattern of the empty thin-walled beams obtained from the numerical simulation is in good agreement with the final deformed shape of the beam in the experiment. A typical behavior of bending deformation is shown from both experiment and simulation: an inward fold at the compression flange and two outward folds at the adjacent flanges. The inward fold and outward fold form a sectional crush zone,

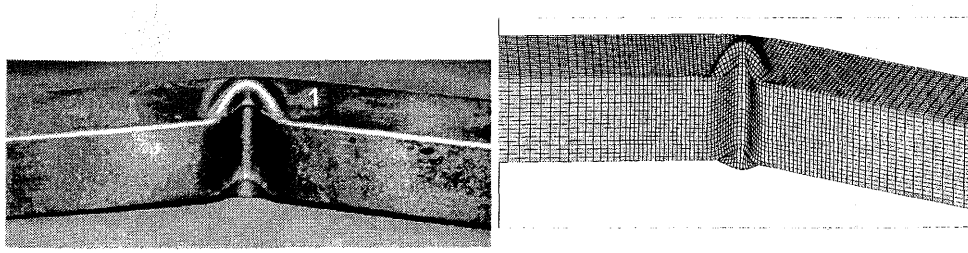

Figure 4: Deformation pattern of empty thin-walled beam

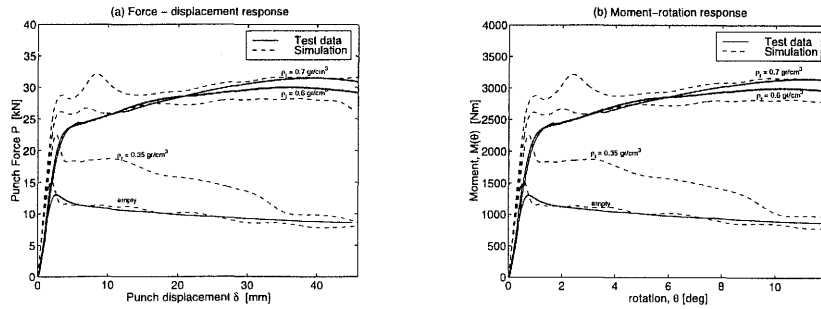

Figure 5: Three point bending response of fully foam–filled beam

which is associated with the decreasing plastic resistance of the thin–walled beam. The decrease of the plastic resistance is shown by the drop of the moment–rotation response in Figure 5.

The localized deformation of the thin–walled beam is characterized by folding length $2H$. Analytically, the half folding length of an empty thin–walled beam can be calculated by using $H = 1.3\, b^{2/3}\, t^{1/3}$, see Ref. [3]. With the cross sectional geometries: width $b = 50\ mm$, and thickness $t = 1.5\ mm$, the analytical folding length of the thin–walled beam is calculated as $2H = 39.6\ mm$. This folding length is in good agreement with the experiment and numerical simulations where the folding length is approximately 40 mm. Note that the localized deformation does not conform the circular shape of the punch, which has diameter of 50 mm. The local punch indentation is only affecting the initial crushing of the beam.

6.2 Full foam filling

The first filling method is studied by inserting the aluminum foam to the entire length of the thin–walled beam. Four different foam densities were considered in addition to the empty beam. No adhesive is introduced, and therefore the strengthening interaction occurs through the sliding interface between the wall and the aluminum foam. The inward fold formations are retarded by the lateral support of the foam which results in higher bending strength.

The punch force – displacement data can be converted into moment – rotation relationship. The resulting moment is the maximum bending moment at the center length of the beam. From the three point bending configuration, the bending moment and the rotation can approximated as, valid for small rotation angles,

$$M = \frac{P\,L}{4} \tag{1}$$

$$\theta = \tan^{-1}\left(\frac{2\,\delta}{L}\right) \tag{2}$$

where P and δ are the punch force and displacement, respectively, while L is the stopper distance (see Figure 2 for test geometry). Figure 5 shows the three point bending response of the fully foam–filled beam. The bending resistance increases significantly due to the presence of the foam filler. For low density foam filling $\rho = 0.35\ g/cm^3$, the force response drops after reaching the ultimate value. In the case of higher foam density ($\rho = 0.6 - 0.835\ g/cm^3$), The load–displacement response is monotonically increasing with the hinge rotation.

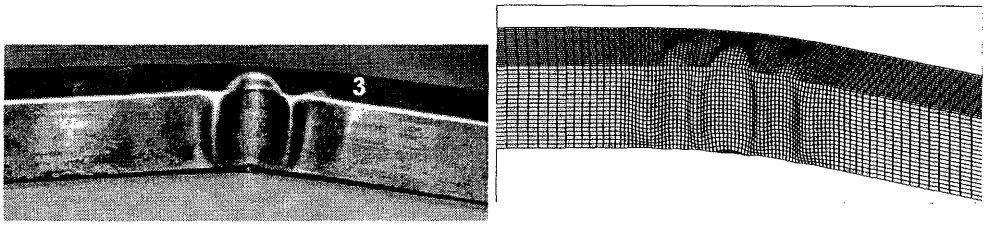

Figure 6: Deformation pattern of fully filled beam with highly dense aluminum foam

The increase of the bending resistance can be explained by observing the deformation pattern of the fully foam–filled beam depicted in Figure 6. It appears that for highly dense foam filling, the localized folding propagates to the adjacent sections rather than reduce the cross section. Therefore, the foam filler forces the beam to form more plastic hinge lines, increase the moment arm of the compression flange, thus maintaining higher bending crush resistance.

6.3 Partial foam filling

Due to the localized nature of bending fold deformation, the concept of filling can be adjusted so that the foam filler is only applied at the localized folding zone. Partial foam filling at the center portion of the beam with five different lengths are simulated, e.g. $L_f = 90,\ 120,\ 190\ mm$. The density of the foam filler used in the simulation was $\rho_f = 0.6\ g/cm^3$. The three point bending response are shown in Figure 7 It shows that the peak force of the partial foam filling is higher for longer foam length. For

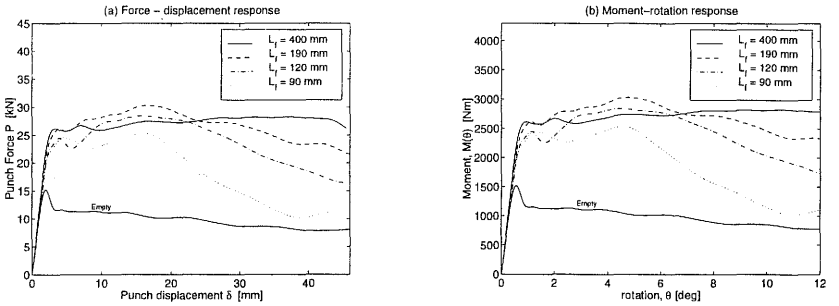

Figure 7: Three point bending response of partial foam filling

short foam length, the load carrying capacity drops after small rotation, while for long foam length, high bending resistance is maintained. The strengthening mechanism can be analyzed by observing the deformation pattern as shown in Figure 8. For long foam length, progressive folding which results in three crush zones are formed, so that high bending resistance is obtained. For short foam length, only one crush zone at the center of the beam is formed, so that the drop in load carrying capacity occurs just like in the empty beam crushing mechanism. In a limiting case, when the foam length is very short, the depth of crush zone formed below the punch is limited and instead a new hinge is formed at the end of the foam length which eliminates the strengthening mechanism of the foam.

The theoretical length of the foam filling can be calculated by considering the beam strength at the

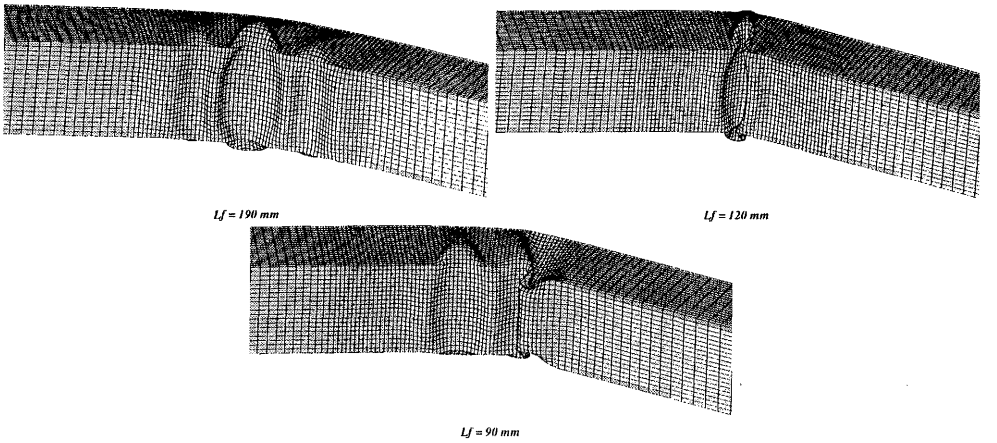

Figure 8: Deformation pattern of partial foam filling

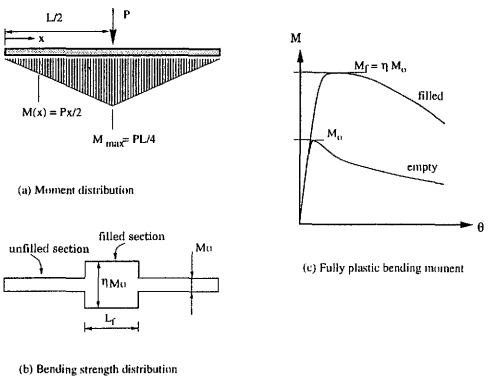

Figure 9: Bending strength and moment distribution of partially foam filled beam

unfilled and filled section, see Figure 9. In the unfilled section, the beam strength is equal to the fully plastic bending moment of an empty beam M_o, while at the filled section, the beam strength is equal to the fully plastic bending moment of filled beam M_f. Defining a scaling parameter $\eta = M_f/M_o$, the distribution of the beam strength becomes M_o at the unfilled section and ηM_o at the filled section with foam length of L_f. The critical foam length can then be obtained by equating the the largest moment at the unfilled section with the maximum moment of the filled section.

$$M_{max} = M_o\eta = \frac{PL}{4} \tag{3}$$

$$M_{x=\frac{L-L_f}{2}} = M_o = \frac{P}{4}(L - L_f) \tag{4}$$

By equating equations (3) and (4), one can obtain the limiting length of the foam filler as

$$L_f = L\left(\frac{\eta - 1}{\eta}\right) \tag{5}$$

Equation 5 sets the minimum length of the foam filler length. If the foam length is greater than L_f, than the foam–beam strengthening mechanism will be obtained. Otherwise, the foam strengthening will not be achieved, instead the folding will occur at the boundary between unfilled and filled sections, and therefore, the bending characteristics will be similar to the empty thin–walled beam.

For the thin–walled beam considered in the simulation, the characteristic geometry strength is as follows: $L = 400\ mm$, and from fully filled foam with $\rho_f = 0.6\ g/cm^3$, the scale factor $\eta = 1.9$, therefore the minimum foam length should be $L_f = 189.5\ mm$. From the deformation pattern shown in Figure 8, the partial filling with the foam length of greater than 177 mm shows that progressive folding is formed and therefore higher bending resistance is achieved. However, partial filling with the foam length of $L_f = 120\ mm$ still gives higher bending resistance and the localized folding still occurs at the center part of the filling. This is due to the effect of folding wave length of the thin–walled beam. Therefore, the effective foam length is proposed as

$$L_{f,eff} = L\left(\frac{\eta - 1}{\eta}\right) - 4H \tag{6}$$

where H is the half folding wave length. With this effective foam length, the minimum foam length for the partial filling will be $L_{f,eff} = 189.5 - 80 = 109.5\ mm$. From Figure 8, it shows that for the foam length $L_f = 90\ mm$, the localized fold is formed at the boundary between the filled and unfilled section. The above comparison proves the usefulness of the simplified equation for the minimum length of the foam–filled section of the beam.

7 Discussion and Conclusion

The experiments and numerical simulations of foam–filled beams have shown significant increase of the bending resistance. The most important results are summarized as follows:

1. The presence of the foam filler change the crushing mode of the thin–walled beam, from one localized fold to multiple propagating folds. This modified mechanism prevents the drop in load carrying capacity due to the formation of more plastic hinge lines, producing a limited sectional crush, and therefore more bending energy can be dissipated.

2. Partial foam filling offers significant reduction of the foam weight while maintaining higher crushing resistance. The effective foam length L_f is developed and should be used as a guideline for designing the partially foam–filled beam. More experiment should be conducted in the case of partially foam–filled beams.

Potential applications of the foam-filled sections are for the automotive structures. The foam-filled section can be used for the front rail and firewall structures to absorb impact energy during frontal collision. In the case of side collision, the foam–filled section can be used to strengthen the B–pillar structure to avoid severe intrusion in the passenger compartment. Furthermore, the foam–filled section can also be used in the A-pillar and roof frame structures to prevent severe roof crush during roll over accident.

Acknowledgments —The present work was supported by the Joint MIT/Industry Consortium on Ultralight Metal Body Structures and the Fraunhofer Institute for Applied Materials Research (IFAM). The financial supports of both sources are gratefully acknowledged. The authors would like to thank to Dr. E. Haug of ESI Paris and Mr. G. Christ of Altair Computing for their continuous support with the finite element programs of PAM CRASH^{TM} and mesh generator program of HYPERMESH.

References

[1] D. Kecman. Bending collapse of rectangular and square section tubes. *Int. J. Mech. Sci.*, 25(9/10), 1983.

[2] I.J. McGregor, D.J. Meadows, C.E. Scott, and A.D. Seeds. Impact performance of aluminum structures. In Jones, N. and Wierzbicki, T., editors, *Structural Crashworthiness and Failure*, pages 385–421. Elsevier, 1993.

[3] T. Wierzbicki, W. Abramowicz, T. Gholami, and L. Recke. Stress profiles in thin-walled prismatic columns subjected to crush loading–II. Bending. *Computers & Structures*, 51(6):pp. 624–640, 1994.

[4] H.D. Kunze, J. Baumeister, J. Banhart, and M. Weber. P/M technology for the production of metal foams. *Powder Metallurgy International*, 25(4):pp. 182–185, 1993.

[5] S.P. Santosa and T. Wierzbicki. Effect of an ultralight metal filler on the bending collapse behavior of thin–walled prismatic columns, 1999. *Technical Report 6*, Impact & Crashworthiness Laboratory, MIT, *International Journal of Mechanical Sciences, Vol. 41, pp. 995–1019, 1999.*

[6] S.P. Santosa and T. Wierzbicki. Crash behavior of box column filled with aluminum honeycomb or foam. *Computers & Structures*, 68(4):343–368, June 1998.

[7] S.P. Santosa, T. Wierzbicki, A.G. Hanssen, and M. Langseth. Experimental and numerical studies of foam–filled sections, 1998. *Technical Report 9*, Impact & Crashworthiness Laboratory, MIT, *International Journal of Impact Engineering (in print).*

[8] J. Banhart and J. Baumeister. Deformation characteristics of metal foams. *Journal of Materials Science*, 33(14):31–44, 1998.

[9] S.P. Santosa. Axial crushing of foam–filled sections: Numerical predictions vs. experiments, 1998. Report No: 9, Impact & Crashworthiness Laboratory, MIT, April 1998.

[10] Santosa, S.P. and Wierzbicki, T. On the modelling of crush behavior of closed–cell aluminum foam structure, 1997. *Technical Report 3*, Impact & Crashworthiness Laboratory, MIT, *Journal of the Mechanics and Physics of Solids, Vol. 46, No. 4, pp. 645–669, 1998.*

[11] L.J. Gibson and M.F. Ashby. *Cellular Solids: Structure and Properties.* Cambridge University Press, Cambridge, UK, 1997.